JOURNAL OF VIROLOGY, Sept. 2003, p. 10060–10070 Vol. 77, No. 18
0022-538X/03/$08.00+0 DOI: 10.1128/JVI.77.18.10060–10070.2003

T Cells Cause Acute Immunopathology and Are Required for Long-Term Survival in Mouse Adenovirus Type 1-Induced Encephalomyelitis

Martin L. Moore,[1] Corrie C. Brown,[2] and Katherine R. Spindler[3]*

Department of Genetics, Franklin College of Arts and Sciences,[1] and Department of Pathology, College of Veterinary Medicine,[2] University of Georgia, Athens, Georgia 30602, and Department of Microbiology and Immunology, University of Michigan Medical School, Ann Arbor, Michigan 48109[3]

Received 9 April 2003/Accepted 17 June 2003

Infection of adult C57BL/6 (B6) mice with mouse adenovirus type 1 (MAV-1) results in dose-dependent encephalomyelitis. Utilizing immunodeficient mice, we analyzed the roles of T cells, T-cell subsets, and T-cell-related functions in MAV-1-induced encephalomyelitis. T cells, major histocompatibility complex (MHC) class I, and perforin contributed to acute disease signs at 8 days postinfection (p.i.). Acute MAV-1-induced encephalomyelitis was absent in mice lacking T cells and in mice lacking perforin. Mice lacking α/β T cells had higher levels of infectious MAV-1 at 8 days, 21 days, and 12 weeks p.i., and these mice succumbed to MAV-1-induced encephalomyelitis at 9 to 16 weeks p.i. Thus, α/β T cells were required for clearance of MAV-1. MAV-1 was cleared in mice lacking perforin, MHC class I or II, $CD4^+$ T cells, or $CD8^+$ T cells. Our results are consistent with a model in which either $CD8^+$ or $CD4^+$ T cells are sufficient for clearance of MAV-1. Furthermore, perforin contributed to MAV-1 disease but not viral clearance. We have established two critical roles for T cells in MAV-1-induced encephalomyelitis. T cells caused acute immunopathology and were required for long-term host survival of MAV-1 infection.

Most insights into adenovirus pathogenesis have come from natural infections because adenoviruses are species specific. A better understanding of how adenoviruses interact with the host immune system would be beneficial because adenoviruses are important human pathogens (30) and because the immune system limits the efficacy of adenovirus-mediated gene therapy (80). In fact, a greater appreciation of the immunogenicity of adenoviruses has led to the use of adenovirus vectors in immunotherapy and therapeutic vaccine strategies (51). Determining how adenoviruses and T cells interact will improve strategies for adenovirus-mediated immunotherapy. Mouse adenovirus type 1 (MAV-1) provides an ideal model system for the investigation of adenovirus-host interactions at the level of immunity.

Study of MAV-1 permits the examination of a replicating adenovirus in vivo. The double-stranded, linear DNA genome of MAV-1 is similar to those of human adenoviruses (hAds) in overall organization (50). The virus causes acute and persistent infections in mice (reviewed in reference 64). Doses of as low as 1 to 100 PFU cause fatal disease in newborn and adult mice, and disease outcomes depend on the dose and strain of virus and the strain of mice infected (24, 45, 56, 66). Inoculation of adult immunocompetent mice with wild-type MAV-1 results in a systemic infection of cells of the mononuclear phagocyte system and endothelial cells of the microvasculature (11, 39). In adult C57BL/6 (B6) mice, this leads to dose-dependent encephalomyelitis (24). Brains of infected mice exhibit perivascular edema, and moribund infected mice also exhibit endothelial cell reactivity, vasculitis, vascular wall degeneration, and viral inclusion bodies (11, 24, 39, 45, 66). Although MAV-1 can be detected in organs throughout the mouse, the highest levels of virus are found in the spleen and central nervous system (45, 63). In situ hybridization and immunohistochemistry have shown that the virus is excluded from B cells and T cells in the spleen (39). The endothelial tropism of MAV-1 is striking: the virus has not been observed in the brain parenchyma and is restricted to the vascular endothelium (11, 24, 39).

The immune response to acute MAV-1 infection involves innate (10), cellular (31, 34), and humoral (14) immunity. By 96 h postinfection (p.i.), brains of B6 mice infected with MAV-1 have increased levels of mRNAs of the cytokines interleukin-1, tumor necrosis factor alpha, lymphotoxin, and interleukin-6; the chemokines IP-10, MCP-1, MIP-1α, MIP-1β, and RANTES; and the chemokine receptors CCR1 to -5 (10, 11). Neutralizing and complement-fixing antibodies are detected at 2 to 3 weeks p.i. in adult mice infected with MAV-1, and antibody titers decline after 24 months (68). Sublethally infected adult mice develop MAV-1-specific cytotoxic T cells (CTL) that are detectable at 4 days p.i., peak at 10 days p.i., and then rapidly decline (31–34). Inbred mouse strains that are resistant and susceptible to MAV-1 have been identified, and sublethal irradiation of resistant C3H/HeJ mice renders them susceptible (66). Taken together, these studies suggest that immune responses are determinants of MAV-1 pathogenesis. However, the role of these processes in MAV-1 disease is largely unexplored.

T cells can limit pathology due to viral infection and/or cause collateral pathological damage in the context of acute (13, 40) and persistent (28, 54) viral infections. The balance between an effective antiviral T-cell response and T-cell-mediated immunopathogy is critical for host survival. The parameters that

* Corresponding author. Mailing address: University of Michigan Medical School, 1150 W. Medical Center Dr., 6724 Medical Science Building II, Ann Arbor, MI 48109-0620. Phone: (734) 615-2727. Fax: (734) 764-3562. E-mail: krspin@umich.edu.

govern this balance vary among virus-host systems (26, 53). However, the kinetics and abundance of viral antigen presentation in secondary lymphoid tissue and the effects of costimulatory host molecules are key determinants of T-cell activation (reviewed in references 36 and 79). Cell-mediated immunity (CMI) describes the effector functions of T cells, and these can be broadly classified into two types: cytotoxicity and cytokine production. αβ $CD8^+$ T cells can undergo differentiation into effector CTL by a major histocompatibility complex (MHC) class I-dependent process, and they deliver cytotoxic granule proteins such as perforin to target cells (reviewed in reference 38). $CD8^+$ T cells can also produce antiviral cytokines (reviewed in reference 25). αβ $CD4^+$ T cells interact with peptide-MHC class II molecules on the surface of antigen presenting cells (APCs) to become potent cytokine producers, and $CD4^+$ effector T cells can have cytotoxic potential (2). γδ T cells are largely double negative for CD4 and CD8, are abundant in epithelial tissues, are excluded from the lymphoid parenchyma, can recognize antigens in the absence of MHC, and can secrete cytokines or mediate cytotoxic cell killing (reviewed in reference 29).

Using available immunodeficient mice, we evaluated the roles of T cells, T-cell subsets, MHC class I, MHC class II, and perforin in protection from and contribution to MAV-1 disease. Mice lacking α/β or α/β and γ/δ T cells were resistant to acute disease, exhibited less acute histopathology than control mice, failed to limit MAV-1 replication, and succumbed at 9 to 16 weeks p.i. Mice lacking MHC class I function were resistant to acute disease signs, although they had higher viral loads than control mice in the acute phase. Mice lacking MHC class I function eventually cleared MAV-1. Mice lacking perforin showed fewer acute disease signs than controls but cleared MAV-1 similarly. No difference between control and MHC class II-deficient mice was detected. Our observations establish two critical roles for T cells in MAV-1-induced encephalomyelitis. T cells contributed to acute immunopathology and were required for long-term host survival of MAV-1-infected mice.

MATERIALS AND METHODS

Virus and mice. Wild-type MAV-1, originally obtained from S. Larsen (5), was grown and passaged in NIH 3T6 fibroblasts, and titers of viral stocks were determined by plaque assay on 3T6 cells as previously described (9). All animal work complied with all relevant federal and institutional policies. C57BL/6J (B6), B6.129S-Tcra^{tm1Mom} (T-cell receptor alpha-negative [$TCR\alpha^{-/-}$]), B6.129P2-Tcrb^{tm1Mom}Tcrd^{tm1Mom} ($TCR\beta x\delta^{-/-}$), B6.129P2-Tcrd^{tm1Mom} ($TCR\delta^{-/-}$), C57BL/6-Pfp^{tm1Sdz} (perforin-negative [$Pfp^{-/-}$]), B6.129S6-Cd4^{tm1Knw} ($CD4^{-/-}$), and B6.129S2-Cd8a^{tm1Mak} ($CD8^{-/-}$) mice were purchased from the Jackson Laboratory. B6.129-Abb^{tm1}N5 (MHC class II-deficient) and B6.129P2-B2m^{tm1}N5 (MHC class I-deficient) mice were purchased from Taconic. C57BL/6NCr (B6) mice were purchased from the National Cancer Institute. In all assays we have done to date on infected B6/J or B6/NCr mice, the two strains have behaved indistinguishably (this work and data not shown). These include survival experiments, viral growth, histopathology, and in situ hybridization. Mice were infected with the indicated doses by the intraperitoneal route in a volume of 0.1 ml of phosphate-buffered saline. Mice were housed in microisolator cages, age and sex matched, and infected at between 4 and 6 weeks of age. Infected mice were scored twice daily for the presence or absence of any disease signs, i.e., hunched posture, ataxia, or ruffled fur, and also, in moribund mice, abdominal breathing, hindlimb paralysis, seizure, or tremor. Moribund mice were euthanatized by CO_2 asphyxiation.

Quantitation of virus from organs. Organs were harvested aseptically from euthanatized mice, and homogenates were prepared as described previously (66). Virus was titrated by plaque assay on 3T6 cells as previously described (9). Briefly, 20 to 200 mg of tissue was homogenized in phosphate-buffered saline in a microcentrifuge tube by using a plastic pestle and sterile sand. Organ homogenates (5 to 10%, wt/vol) were serially diluted and assayed. The means of the log titers were compared by a two-tailed *t* test, assuming equal variance. Counts of fewer than 20 plaques per 60-mm-diameter plate were considered unreliable. Therefore, 2×10^3 PFU/g of tissue was calculated as the detection limit. Values below the detection limit were excluded from statistical analyses (calculations of means and *t* test statistics).

Histology. The following organs were harvested and fixed in 10% formalin: spleen, kidney, liver, small and large intestines, Peyer's patches, mandibular lymph nodes, thymus, lung, heart, and brain. Tissues were formalin fixed and paraffin embedded as previously described (39). Hematoxylin and eosin (H-E)-stained sections were viewed by light microscopy.

ISH. In situ hybridization (ISH) was performed as previously described (39). Briefly, sections were deparaffinized, rehydrated, digested with proteinase K, and probed with an antisense digoxigenin riboprobe transcribed from a segment of the E3 region inserted into pBluescript SK(−) vector. Following hybridization, slides were incubated with antidigoxigenin-alkaline phosphatase (Boehringer Mannheim), and the substrate nitroblue tetrazolium plus 5-bromo-4-chloro-3-indolylphosphate (Boehringer Mannheim) was added. Slides were lightly counterstained with hematoxylin, and coverslips were applied with Permount.

PCR and reverse transcription-PCR (RT-PCR). For DNA isolation, approximately 50 mg of tissue was incubated overnight at 55°C in 700 μl of 50 mM Tris (pH 8.0)–100 mM EDTA–100 mM NaCl–1% sodium dodecyl sulfate–0.5 mg of proteinase K per ml. Samples were mixed with an equal volume of phenol and then centrifuged at 18,400 × *g* for 5 min at room temperature. The aqueous layer was mixed with an equal volume of chloroform-isoamyl alcohol (24:1). The aqueous layer was precipitated with 95% ethanol and washed once with 70% ethanol. The pellets were air dried and resuspended in 100 μl of 0.1× SSC (1× SSC is 0.15 M NaCl plus 0.015 M sodium citrate) at 65°C. For RNA isolation, approximately 50 mg of harvested tissue stored in RNAlater (Ambion) was homogenized in 900 μl of TRI reagent (Molecular Research Center, Inc.) at room temperature in a microcentrifuge tube by using sterile sand and a plastic pestle. Sand and tissue debris were removed by centrifugation (5 min, 700 × *g*), and RNA was isolated according to the manufacturer's instructions. Positive control RNA was prepared as previously described (8) from 3T6 fibroblasts infected with MAV-1 at a multiplicity of infection of 5.

For PCR analysis, 1 μg of DNA obtained from spleen or brain was used as the template in a 55-cycle reaction. Reaction conditions and the MAV-1 E3-specific primers MAVR24718 and MAVR25148 were as described previously (66). For RT-PCR analysis, spleen and brain RNAs were reverse transcribed with avian myeloblastosis virus reverse transcriptase as previously described (6) and PCR amplified in a 35-cycle reaction. MAVR24718 and MAVR25148 span an E3 intron and therefore can be used to distinguish cDNA from any contaminating genomic DNA. PCR and RT-PCR products were visualized on 7% polyacrylamide gels.

RESULTS

Virulence of acute MAV-1 infection in B6 and mutant mouse strains. Since in various virus-host systems T cells can be important for viral clearance and can cause immunopathology, we wanted to determine whether the clinical outcome of MAV-1 infection was altered in T-cell-deficient mice. Mice were infected intraperitoneally at various doses and monitored for disease signs and mortality at 8 days p.i. This time point corresponds to the acute phase of infection. The dose-dependent mortality of control mice listed in Table 1 agrees with published MAV-1 50% lethal doses for B6 mice (24, 66). $TCR\alpha^{-/-}$ mice lack α/β T cells, and $TCR\beta x\delta^{-/-}$ mice lack both α/β and γ/δ T cells (52). Unlike MAV-1-infected control mice, MAV-1-infected $TCR\alpha^{-/-}$ and $TCR\beta x\delta^{-/-}$ mice exhibited no clinical disease signs up to 8 days p.i. at all doses tested (Table 1). Also, $TCR\beta x\delta^{-/-}$ mice infected with 10^4 PFU of MAV-1 exhibited 100% survival at 8 days p.i., in contrast to control mice (Table 1). To dissect what α/β T-cell function could be contributing to MAV-1 disease, we infected mice deficient in certain T-cell subsets and CMI functions. α/β T-cell development depends on the surface expression of MHC molecules (23, 44, 59). Mice with a targeted mutation of the

TABLE 1. Virulence of MAV-1 at 8 days p.i.

Mouse strain (abbreviation)	Deficiency	Intraperitoneal dose (PFU)	No. of mice with signs of disease[a] at 8 days p.i.[b]	Survival at 8 days p.i.[b]
C57BL/6J (B6), C57BL/6NCr (B6)	None	100	1/12	12/12
		700	46/54	49/54
		10^4	5/5	2/5
B6.129S-Tcra$^{tm/Mom}$ (TCR$\alpha^{-/-}$)	T cells (TCRα)	100	0/6	6/6
		700	0/3	ND[c]
B6.129P-Tcrb$^{tm/Mom}$Tcrd$^{tm/Mom}$ (TCRβx$\delta^{-/-}$)	T cells (TCRβ, δ)	700	0/16	16/16
		10^4	0/5	5/5
B6.129-Abb^{tml} N5 (MHC class II deficient)	MHC class II, CD4$^+$ T cells	700	7/9	8/9
B6.129P2-B2m$^{tm/Unc}$ (MHC class I deficient)	MHC class I, CD8$^+$ T cells	700	0/6	6/6
C57BL/6-Pfp$^{tm/Sdz}$ (Pfp$^{-/-}$)	Perforin	10^4	0/8	8/8

[a] Hunched posture, ataxia, or ruffled fur; also, in moribund mice, abdominal breathing, hindlimb paralysis, seizure, or tremor.
[b] The cumulative disease signs and survival for multiple B6 control infections are indicated. The number of B6 mice used as proximate controls for each of the mutant mouse strains was as follows: TCR$\alpha^{-/-}$, 100 PFU, $n = 3$; TCR$\alpha^{-/-}$, 700 PFU, $n = 3$; TCRβx$\delta^{-/-}$, 700 PFU, $n = 18$; TCRβx$\delta^{-/-}$, 10^4 PFU, $n = 5$; MHC class II deficient, $n = 9$; MHC class I deficient, $n = 6$; Pfp$^{-/-}$, $n = 8$.
[c] ND, not determined.

MHC class II A^b_β gene have a deficiency in CD4$^+$ T cells and MHC class II-dependent CMI (23). Mice with a targeted disruption of the β_2-microglobulin (β_2m) gene are deficient in CD8$^+$ T cells and MHC class I-dependent CMI (44). $\beta_{2m}{}^{-/-}$ mice are also deficient in CD1 expression and lack NKT cells (7, 12). ($A^{b-/-}_\beta$ and $\beta_{2m}{}^{-/-}$ mice will hereafter be referred to according to their primary deficiencies, i.e., MHC class II and I, respectively, although these mice have deficiencies in specific T-cell subsets. We acknowledge that the immunodeficient mice used in these studies may also have other, uncharacterized phenotypes that could alter MAV-1 pathogenesis.) There was no difference in the proportion of survival between control and MHC class II-deficient mice, and they had similar disease signs (Table 1). In contrast, MHC class I-deficient mice showed no disease signs up to 8 days p.i. (Table 1). We tested the role of perforin, a cytolytic pore-forming protein known to be secreted by effector CD8$^+$ T cells (20), CD4$^+$ T cells (2, 72), and NK cells (62). Mice lacking perforin (Pfp$^{-/-}$) were resistant to acute MAV-1 disease, showing no disease signs or mortality at 8 days p.i. (Table 1). Together, the observations with mice lacking perforin, MHC class I function, and T cells indicate that acute MAV-1 disease is dependent on MHC class I and lymphocyte-mediated cytotoxicity.

Quantitation of infectious virus from organs of acutely infected B6 and mutant mouse strains. We tested whether the altered virulence of MAV-1 in immunodeficient mice compared to B6 controls correlated with the level of virus replication in tissues of MAV-1-infected mice. MAV-1 replicates to highest levels in the spleen and central nervous system (39, 45). We harvested spleens and brains of infected mice and titrated infectious virus by plaque assay. There was no difference in viral titers in spleens and brains between B6 mice and mice lacking α/β T cells at 6 days p.i. (Fig. 1A) or in mice lacking α/β and γ/δ T cells at 7 days p.i (Fig. 1B). Figure 1C shows that at 8 days p.i. viral titers in spleens and brains of mice lacking α/β T cells were higher than those in B6 mice. Similar to the T-cell-deficient mice assayed at 8 days p.i. for Table 1, the T-cell-deficient mice for Fig. 1 exhibited no disease signs at 6 to 8 days p.i., whereas control mice exhibited typical dose-dependent MAV-1 disease signs (Table 1 and data not shown). We tested the role of MHC class I in limiting MAV-1 replication. Figure 1D shows that at 8 days p.i. levels of infectious virus were the same in spleens of MHC class I-deficient and B6 mice, but there was more virus in the brains of MHC class I-deficient mice ($P = 0.03$). We tested the role of perforin in limiting MAV-1 replication. Figure 1E shows that perforin did not play a role in control of MAV-1 replication at 8 days p.i., because levels of virus were the same in spleens and brains of control and Pfp$^{-/-}$ mice. We tested whether MHC class II has a role in limiting MAV-1 replication. At 9 days p.i., there was no detectable infectious virus in MHC class II-deficient or B6 spleens and brains (data not shown), suggesting that control of MAV-1 in the acute phase does not depend on MHC class II. Together the data indicate that control of acute MAV-1 replication was T-cell dependent but perforin and MHC class II independent.

Histopathology and ISH analysis of acutely infected T-cell-deficient, perforin-deficient, and control mice. Since T-cell- and perforin-deficient mice had altered MAV-1 disease phenotypes compared to B6 controls (Table 1), we assessed the histological evidence of MAV-1 disease in these mice. Figure 2A to D show representative histopathology and ISH of brain sections of B6 and TCRβx$\delta^{-/-}$ mice infected with 700 PFU and harvested at 7 days p.i. (same mice as for Fig. 1B). In infected B6 mice there was perivascular edema, vascular wall degeneration, and small numbers of inflammatory cells in the brain (Fig. 2A). In contrast, the microvasculature of infected TCRβx$\delta^{-/-}$ brains appeared to be normal (Fig. 2C). This strongly suggests that T cells mediate acute immunopathology in the brain. H-E staining of mock-infected B6 brain is shown in Fig. 2E. Mock-infected brains of all strains in Fig. 2 had a similar appearance (data not shown). We assessed the cell tropism of MAV-1 in the presence and absence of T cells by an ISH assay. Figure 2B and D show that there was similar ISH staining of viral nucleic acid in brain microvascular endothelial cells of both control and TCRβx$\delta^{-/-}$ mice. Similarly, in other tissues no difference in cell tropism between control and TCRβx$\delta^{-/-}$ mice was observed (data not shown). Figures 2E to L show histopathology and ISH of brains sections from B6 and Pfp$^{-/-}$ mice mock infected or infected with 10^4 PFU of MAV-1 and harvested at 8 days p.i. (same mice as for Fig. 1E). In infected Pfp$^{-/-}$ brains, there was minimal inflammation

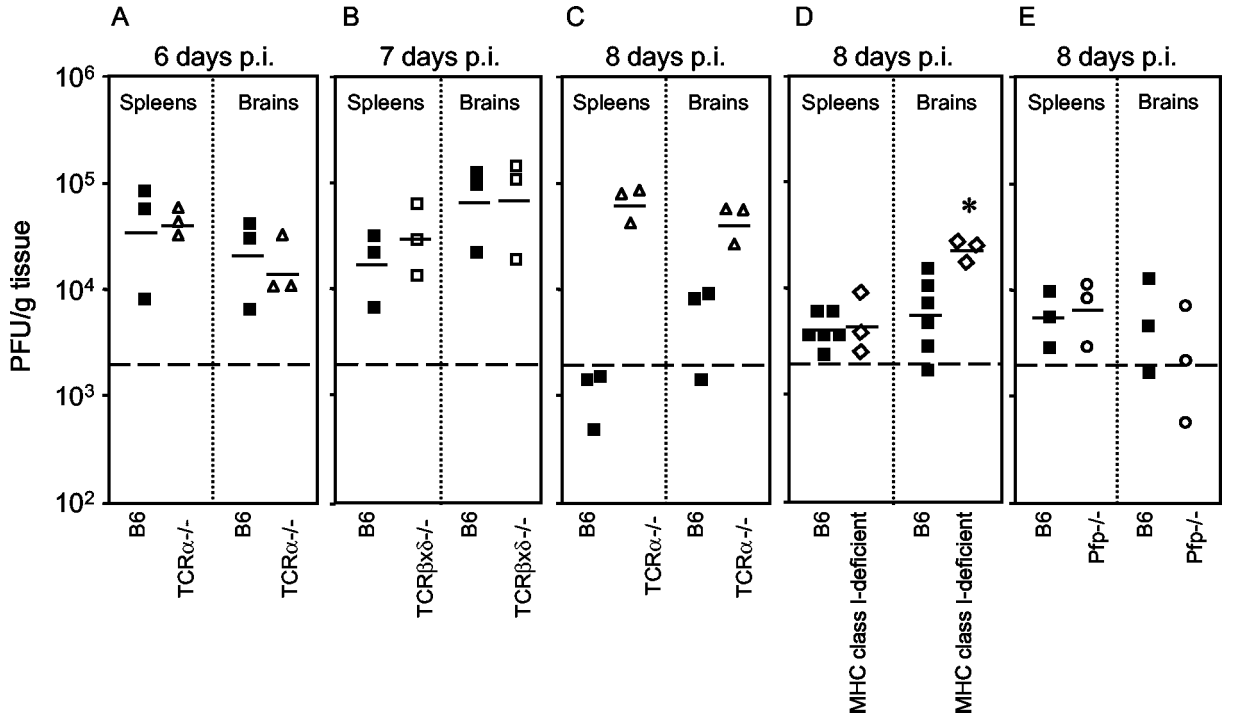

FIG. 1. Quantitation of virus from organs of acutely infected immunodeficient and control mice. Organs were homogenized, and virus was titrated by plaque assay. Each symbol represents an individual mouse. The short horizontal lines represent the means of the log-transformed titers. The dotted line at 2×10^3 represents the lower limit of detection of the assay. (A) Spleens and brains obtained at 6 days p.i from B6 (■) and TCR$\alpha^{-/-}$ (△) mice infected with 10^4 PFU of MAV-1; (B) spleens and brains obtained at 7 days p.i. from B6 (■) and TCR$\beta x\delta^{-/-}$ (□) mice infected with 700 PFU of MAV-1; (C) spleens and brains obtained at 8 days p.i. from B6 (■) and TCR$\alpha^{-/-}$ (△) mice infected with 700 PFU of MAV-1; (D) spleens and brains obtained at 8 days p.i. from B6 (■) and MHC class I-deficient (◇) mice infected with 700 PFU of MAV-1; (E) spleens and brains obtained at 8 days p.i. from B6 (■) and Pfp$^{-/-}$ (○) mice infected with 10^4 PFU of MAV-1. Data points below the limit of detection were excluded when calculating mean titers and *t* statistics. *, $P = 0.03$ compared to titers in B6 brain.

(Fig. 2G). In contrast, the microvasculature of infected B6 brains exhibited large numbers of inflammatory cells, perivascular edema, and vascular wall degeneration (Fig. 2I, K, and L). Brain endothelial cell staining for MAV-1 nucleic acid was not different between control and Pfp$^{-/-}$ mice at 8 days p.i., indicating that there was no difference in the cell tropism of MAV-1 between these mice (Fig. 2H and J). Taken together, the data show that acute MAV-1 encephalomyelitis correlated with the presence of T cells and perforin and not with the level of infectious virus (Fig. 1B and E and 2A to L).

Long-term infection of T-cell-deficient mice. Mice lacking α/β or α/β and γ/δ T cells succumbed to MAV-1 infection at 9 to 16 weeks p.i. (Fig. 3). Moribund T-cell-deficient mice exhibited typical signs of MAV-1 encephalomyelitis, such as ataxia, ruffled fur, hindlimb paralysis, and tremor. Interestingly, all MHC class II-deficient, MHC class I-deficient, and Pfp$^{-/-}$ mice that survived the acute phase of MAV-1 infection survived past 12 weeks p.i. and showed no disease signs (data not shown). To directly assess the contribution of CD4$^+$ and CD8$^+$ T cells to protection from MAV-1, we infected CD4$^{-/-}$ mice and CD8$^{-/-}$ mice. These mice did not succumb to MAV-1 infection; they survived to 12 weeks p.i. (Fig. 3C). Figure 3D shows that mice lacking α/β T cells succumbed to MAV-1 infection at 9 to 15 weeks p.i., whereas mice lacking γ/δ T cells survived. Thus, α/β T cells were required for long-term survival of MAV-1 infection, but γ/δ T cells, perforin, MHC class I function, MHC class II function, CD8$^+$ T cells, and CD4$^+$ T cells were not.

Replication of MAV-1 in long-term-infected T-cell-deficient mice and persistence of MAV-1 in B6 mice. We determined the level of infectious virus in long-term-infected T-cell-deficient mice. High levels of virus were detected in spleen and brain at 3 weeks p.i. in TCR$\alpha^{-/-}$, mice relative to undetectable infectious virus in organs of B6 mice (Fig. 4A). Figure 4B shows titration of infectious virus from the TCR$\beta x\delta^{-/-}$ mice shown in Fig. 3A that were euthanized when moribund at 9 to 12 weeks p.i. Attempts to isolate infectious virus from organs of long-term-infected B6, MHC class II-deficient, and MHC class I-deficient mice yielded no plaques even when organ homogenates were blind passaged sequentially two to three times on 3T6 cells (data not shown). Figure 4C shows quantitation of infectious virus from spleens and brains of mice surviving to 12 weeks p.i. and shown in Fig. 3C. No infectious virus was recovered from B6, CD8$^{-/-}$, and CD4$^{-/-}$ mice, whereas high titers were recovered from the two surviving TCR$\beta x\delta^{-/-}$ mice. Although infectious MAV-1 was undetectable in B6 mice at 12 weeks p.i., we used PCR to assay B6 brains and spleens for MAV-1 DNA and mRNA at 12 weeks p.i. Figure 5 shows the presence of MAV-1 DNA and early region 3 (E3) MAV-1 mRNA in B6 mice at 12 weeks p.i. Thus, in spleens and brains of B6 mice, MAV-1 DNA persists, but if infectious virus is produced, it is not lethal. In contrast, virus replicates to high

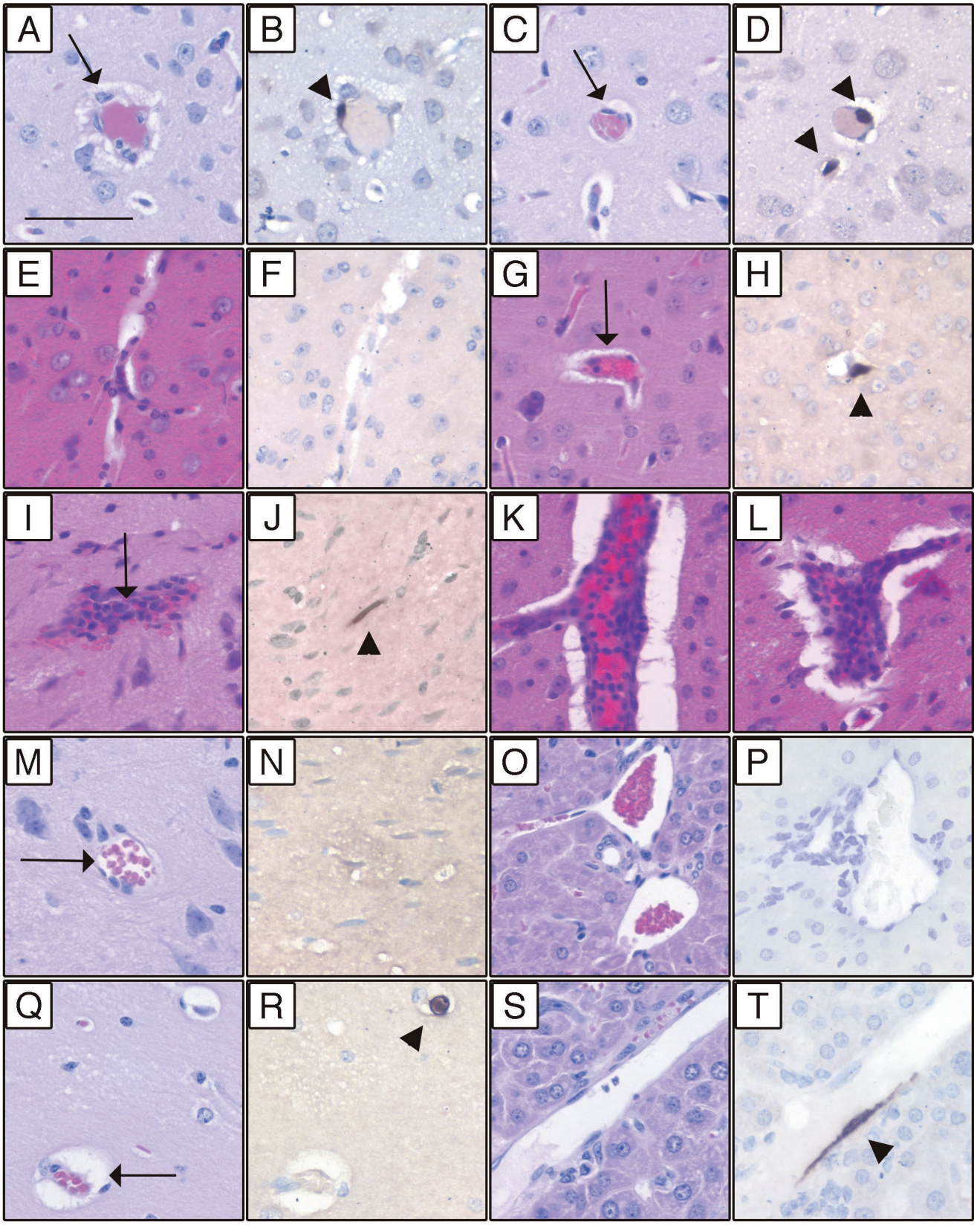

FIG. 2. Histopathology and ISH of infected mice. Sequential sections from paraffin-embedded tissues were stained with H-E or processed for ISH. (A to D) Brains were harvested at 7 days p.i. from B6 and TCRβxδ$^{-/-}$ mice infected with 700 PFU of MAV-1. Shown are sequential H-E- and ISH-stained sections, respectively, of B6 (A and B) and TCRβxδ$^{-/-}$ (C and D) mice. Note the perivascular fibrin deposition and edema in

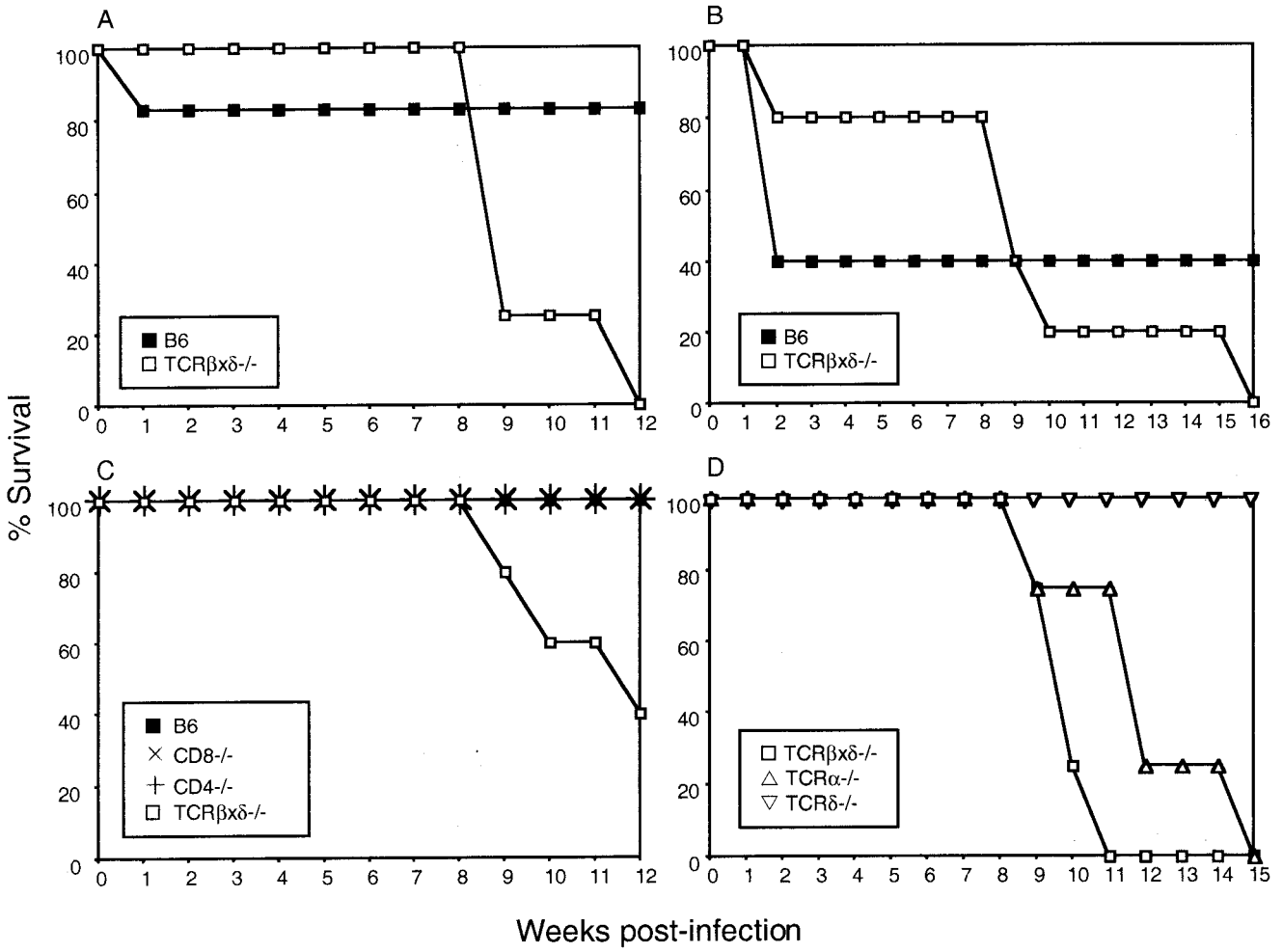

FIG. 3. Susceptibility of B6, TCRβxδ$^{-/-}$, CD8$^{-/-}$, CD4$^{-/-}$, TCRα$^{-/-}$, and TCRδ$^{-/-}$ mice to MAV-1. (A) B6 (n = 6) and TCRβxδ$^{-/-}$ (n = 4) mice were infected with 700 PFU of MAV-1, and survivors were euthanatized at 12 weeks p.i. (B) B6 (n = 5) and TCRβxδ$^{-/-}$ (n = 5) mice were infected with 10^4 PFU of MAV-1 and survivors were euthanatized at 16 weeks p.i. (C) B6 (n = 5), CD8$^{-/-}$ (n = 5), CD4$^{-/-}$ (n = 4), and TCRβxδ$^{-/-}$ (n = 5) mice were infected with 700 PFU of MAV-1, and survivors were euthanatized at 12 weeks p.i. (D) TCRβxδ$^{-/-}$ (n = 4), TCRα$^{-/-}$ (n = 4), and TCRδ$^{-/-}$ (n = 4) mice were infected with 100 PFU of MAV-1, and survivors were euthanatized at 15 weeks p.i.

levels and is lethal in mice lacking α/β T cells (both TCRα$^{-/-}$ and TCRβxδ$^{-/-}$ mice).

Histopathology and ISH analysis of long-term-MAV-1-infeced T-cell-deficient and control mice. Fig. 2M to T show histopathology and ISH of brain and liver sections from B6 and TCRβxδ$^{-/-}$ mice infected with 700 PFU of MAV-1 and euthanatized at 12 weeks p.i. (same mice as for Fig. 3C and 4C). There was no histological evidence of disease or MAV-1 nucleic acid as detected by ISH in B6 brains (Fig. 2M and N) and livers (Fig. 2O and P). There was also no histological evidence of disease or positive ISH staining in CD4$^{-/-}$ mice and CD8$^{-/-}$ mice at 12 weeks p.i. (data not shown). In contrast, there was evidence of typical MAV-1 encephalomyelitis in the brains of TCRβxδ$^{-/-}$ mice (Fig. 2Q), and viral nucleic acid was observed in brain endothelial cells by ISH (Fig. 2R). The livers of B6 and TCRβxδ$^{-/-}$ mice appeared to be histologically normal (Fig. 2O and S). However, MAV-1 nucleic acid was detectable in liver endothelial cells of TCRβxδ$^{-/-}$ mice at 12

B6 (A) but not TCRβxδ$^{-/-}$ (C) brain (arrows). ISH of B6 (B) and TCRβxδ$^{-/-}$ (D) mice showed equivalent positive brown staining of viral nucleic acid in vascular endothelial cells with a MAV-1 probe (arrowheads). (E to L) Brains were harvested at 8 days p.i. from B6 and Pfp$^{-/-}$ mice mock infected or infected with 10^4 PFU of MAV-1. Shown are sequential H-E- and ISH-stained sections, respectively, from mock-infected B6 (E and F), MAV-1-infected Pfp$^{-/-}$ (G and H), and MAV-1-infected B6 (I and J) mice. Note the presence of inflammatory cells in infected B6 (I) but not Pfp$^{-/-}$ (G) brain (arrows). Note equivalent ISH (positive brown staining) of vascular endothelial cells stained with a MAV-1 probe in B6 (J) and Pfp$^{-/-}$ (H) mice (arrowheads). (K and L) Additional H-E-stained B6 brain sections showing severe inflammation and vascular pathology. (M to T) Brains and livers were harvested at 12 weeks p.i. from B6 and TCRβxδ$^{-/-}$ mice infected with 700 PFU of MAV-1. Shown are sequential H-E- and ISH-stained sections, respectively, from B6 brain (M and N), B6 liver (O and P), TCRβxδ$^{-/-}$ brain (Q and R), and TCRβxδ$^{-/-}$ liver (S and T). MAV-1-induced encephalomyelitis is apparent in the TCRβxδ$^{-/-}$ but not the B6 brain (arrows). Note positive MAV-1 ISH of vascular endothelial cells present in TCRβxδ$^{-/-}$ (R and T) but not B6 (N and P) mice (arrowheads). Bar, 50 μm.

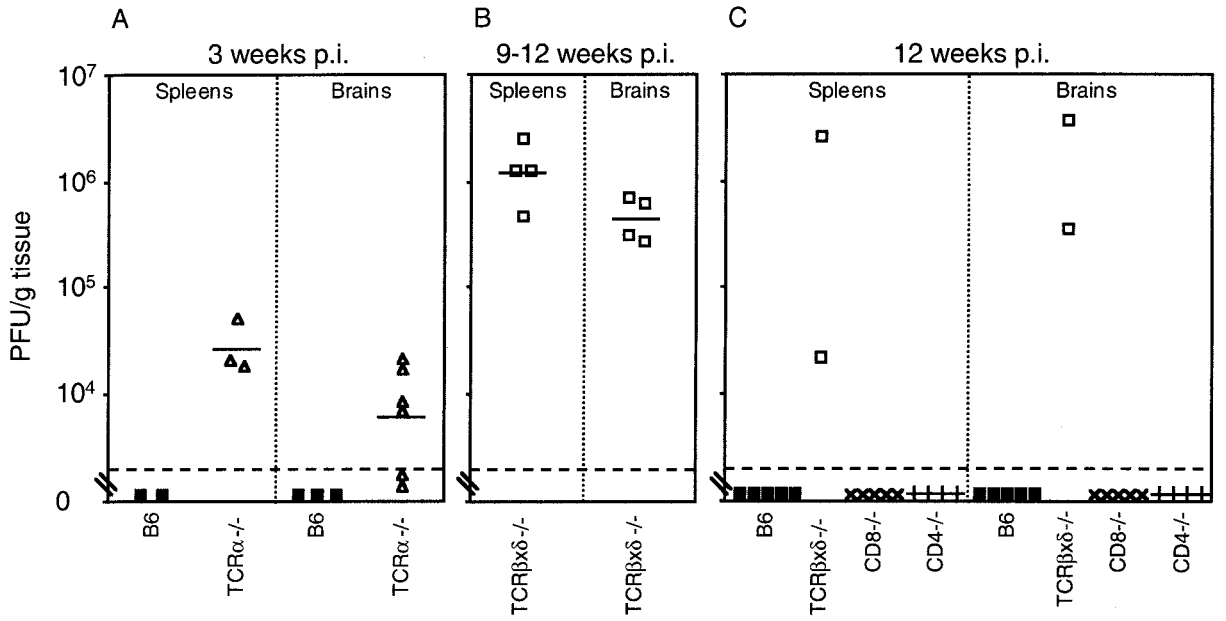

FIG. 4. Replication of MAV-1 in T-cell-deficient mice. (A) Quantitation of virus from spleens and brains obtained at 21 days p.i. from B6 (■) and TCR$\alpha^{-/-}$ (△) mice infected with 100 PFU of MAV-1. (B) Quantitation of virus from spleens and brains obtained at 9 to 12 weeks p.i. from moribund TCRβx$\delta^{-/-}$ mice infected with 700 PFU of MAV-1. (C) Quantitation of virus from spleens and brains obtained at 12 weeks p.i. from B6 (■), TCRβx$\delta^{-/-}$ (□), CD8$^{-/-}$ (×), and CD4$^{-/-}$ (+) mice infected with 700 PFU of MAV-1. Virus levels were determined and are depicted as described in the legend to Fig. 1. Data points below the limit of detection were excluded in calculating mean titers and *t* statistics.

weeks p.i., indicating disseminated MAV-1 replication in the absence of T cells (Fig. 2T).

DISCUSSION

This study was undertaken to determine the roles of T cells in MAV-1-induced encephalomyelitis. We have analyzed the pathogenesis of MAV-1 in mice deficient in T cells, T-cell subsets, and T-cell-related functions. Our results demonstrate that α/β T cells and perforin contribute to acute MAV-1 encephalomyelitis and that α/β T cells are required for control of MAV-1 replication and long-term survival of infection. Our data suggest that mechanisms contributing to T-cell-mediated disease and T-cell-mediated clearance of MAV-1 are different.

CTL were implicated in contributing to disease severity in the acute phase of MAV-1 infection. Since α/β T-cell-deficient, α/β and γ/δ T-cell-deficient, MHC class I-deficient, and perforin-deficient mice were resistant to acute MAV-1 disease, whereas MHC class II-deficient mice were not resistant to MAV-1 disease (Table 1), we reason that CD8$^+$ CTL contributed to acute disease. Experiments to directly test this hypothesis and to assess the role of NK cells in perforin-mediated acute MAV-1 disease are in progress.

Mice with T cells had immunopathology in acute MAV-1 infection that was manifested as encephalomyelitis, and this was not seen in T-cell-deficient mice. Histological evidence of disease in MAV-1-infected B6 mice and the absence of such evidence in MAV-1-infected T-cell-deficient mice correlated with disease signs and not with viral titers (Fig. 1B, 2A, and 2C). Furthermore, at 7 days p.i. endothelial cell staining of viral nucleic acid in the brain was similar for control and TCRβx$\delta^{-/-}$ animals (Figs. 2B and D). Thus, at 7 days p.i. mice without T cells had no acute disease but had levels of infectious MAV-1 and endothelial infection similar to those in mice with a normal T-cell compartment.

Perforin clearly contributed to immunopathology and disease but did not play a role in limiting MAV-1 replication. Pfp$^{-/-}$ mice exhibited less MAV-1-induced encephalomyelitis and showed fewer disease signs than control mice at 8 days p.i. (Table 1; Fig. 2G and I). Perforin-deficient mice, like TCRβx$\delta^{-/-}$ and control mice, had brain endothelial staining for viral nucleic acid (Fig. 2H and J). Levels of infectious MAV-1 were the same in spleens and brains of Pfp$^{-/-}$ and control mice at 8 days p.i. (Fig. 1E), and no infectious virus was recovered from Pfp$^{-/-}$ and control spleens and brains at 24 weeks p.i. (data not shown). The role of perforin in MAV-1-induced encephalomyelitis may be similar to the role of perforin in coxsackievirus B3 (CVB3)-induced myocarditis. Perforin-deficient mice are resistant to acute CVB3 disease and exhibit less myocarditis and inflammatory cell infiltration than controls, but perforin plays no role in clearance of CVB3 (21). This similarity in the pathogenesis of CVB3 and MAV-1 is intriguing because both viruses infect endothelial cells. That Pfp$^{-/-}$ mice exhibit reduced cellular inflammation in response to MAV-1 (Fig. 2G and I) and CVB3 (21) compared to controls suggests that perforin may mediate inflammatory cell recruitment. Perforin may be less important for control of lytic viruses than for control of nonlytic viruses (38). Our results with MAV-1 support this hypothesis. Although MAV-1 is cytopathic in vitro (27), it can replicate to high titers in vivo in the absence of T cells without extensive cellular damage (this report).

MHC class I-deficient mice had statistically higher levels of infectious MAV-1 than control mice in brains but not spleens at 8 days p.i. (Fig. 1D). However, the effect of MHC class I deficiency on viral load was transient, because MHC class

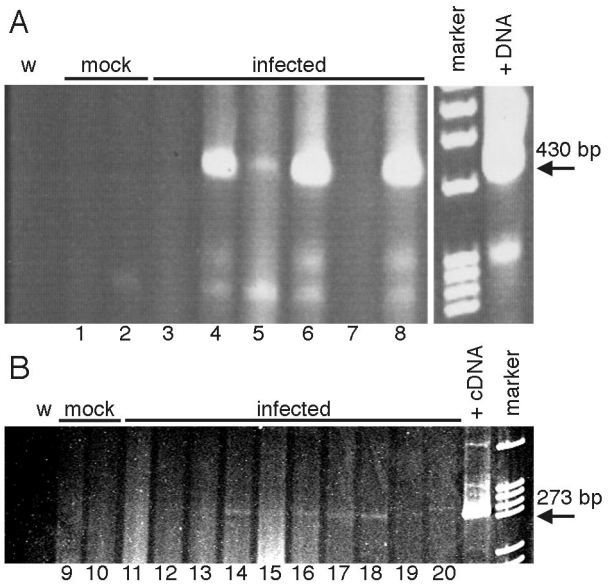

FIG. 5. Presence of MAV-1 nucleic acid in B6 mice at 12 weeks p.i. (A) DNA was isolated from spleens (odd-numbered lanes) and brains (even-numbered lanes) of B6 mice mock infected or infected with 100 PFU of MAV-1 and was analyzed by PCR with MAV-1 E3-specific primers MAVR24718 and MAVR25148 for 55 cycles. The positive DNA control template (+DNA) was 1 μg of DNA isolated from an acutely infected mouse brain known to be positive for infectious virus, and the negative control was water (w). The arrow indicates the 426-bp PCR product from viral DNA. (B) RNA was isolated from spleens (odd-numbered lanes) and brains (even-numbered lanes) of B6 mice mock infected or infected with 700 PFU of MAV-1 and analyzed by RT-PCR with MAV-1 E3-specific primers MAVR24718 and MAVR25148 for 35 cycles. The positive cDNA control template (+cDNA) was from RNA isolated at 20 h p.i. from mouse 3T6 fibroblasts infected with MAV-1 at a multiplicity of infection of 5, and the negative control was water (w). The arrow indicates the 269-bp PCR product from viral cDNA. Each spleen and brain pair (lanes 1 and 2, 3 and 4, etc.) corresponds to a single animal.

I-deficient mice cleared the virus by 12 weeks p.i. (data not shown). Resistance to acute disease and delayed but effective viral clearance from the brain have also been observed in MHC class I-deficient mice infected with neuroadapted Sindbis virus (43). Our data suggest that mechanisms limiting MAV-1 replication in the brain and spleen may differ. MAV-1 infects cells of the monocyte/macrophage lineage and endothelial cells of the microvasculature (24, 39). In spleens, MAV-1-infected cells identified by ISH or immunohistochemistry are more often macrophages than endothelial cells, whereas in brains, the MAV-1-infected cells are always endothelial (M. L. Moore, C. C. Brown, and K. R. Spindler, unpublished data). Further experiments are needed to clarify the role of MHC class I in limiting acute MAV-1 replication.

MHC class II was not required for control of viral load in MAV-1-infected mice. Like control mice, MHC class II-deficient mice cleared infectious MAV-1 by 9 days p.i. (data not shown). We know that MHC class II expression is required for antiviral immunoglobulin G detected at 12 weeks p.i. (M. L. Moore and K. R. Spindler, unpublished data). However, MHC class II-deficient and $CD4^{-/-}$ mice did not differ from controls in disease severity or levels of infectious virus in acute or long-term infection (Table 1 and data not shown). Taken together, the data on T cells, perforin, and MHC class I and II strongly suggest that $CD8^+$ CTL contribute to immunopathology by a perforin-dependent mechanism in acute MAV-1 encephalomyelitis.

Chemokine expression may mediate CTL responses and immunopathology in MAV-1-induced disease. Guida et al. showed that MAV-1 causes encephalomyelitis in B6 mice but not in BALB/c mice (24). Charles et al. then showed that brains and spleens of MAV-1-infected B6 mice have higher levels of chemokine and mRNA expression than brains and spleens of MAV-1-infected BALB/c mice (10). In that report, at 3 and 4 days p.i. the chemokine RANTES was highly expressed in MAV-1-infected B6 brains but was expressed at lower levels in MAV-1-infected BALB/c brains. We have also detected upregulated RANTES expression in B6 brains but not BALB/c brains at 9 days p.i. (Moore and Spindler, unpublished data). The chemokine RANTES attracts T cells and monocytes to sites of inflammation and is required for T-cell function (48). RANTES has been shown to contribute to immunopathology in mouse hepatitis virus-infected mice (46). We hypothesize that the differential chemokine responses between B6 and BALB/c mice result in an immunopathological T-cell response in B6 mice that does not occur in BALB/c mice.

α/β T cells were required for long-term survival of MAV-1 infection. Although α/β T cells contributed to early pathology through a perforin-dependent mechanism, α/β T-cell deficiency resulted in uncontrolled viral replication and eventual death. Thus, a regulated T-cell response is crucial for control of MAV-1 without pathology. $TCR\beta x\delta^{-/-}$ and $TCR\alpha^{-/-}$ mice, both lacking α/β T cells, succumbed to MAV-1 encephalomyelitis 9 to 16 weeks p.i. (Fig. 2Q and 3). MAV-1 was present at high levels in mice lacking α/β T cells (Fig. 1C and 4). In contrast, MHC class I-deficient, MHC class II-deficient, $Pfp^{-/-}$, $CD8^{-/-}$, $CD4^{-/-}$, and $TCR\delta^{-/-}$ mice survived past 12 weeks (Fig. 3C and D and data not shown), and infectious MAV-1 was undetectable from these strains of mice at 12 weeks p.i., even when organ homogenates were serially passaged on 3T6 cells (Fig. 4C and data not shown). It is likely that either $CD8^+$ T cells or $CD4^+$ T cells alone are sufficient for clearance of MAV-1. $CD4^+$ T-cell-independent activation of $CD8^+$ T cells has been experimentally demonstrated (70). An alternative hypothesis is that control of MAV-1 replication requires α/β T cells that express neither CD8 nor CD4. It has been suggested that double-negative ($CD8^-$ $CD4^-$) α/β T cells contribute to immunity to influenza virus in CD4-deficient mice (60).

One interpretation of the role of T cells in MAV-1 pathogenesis is that in the absence of α/β T cells, acute MAV-1 replication is not limited during the acute phase, and MAV-1 continues to replicate productively without causing morbidity and mortality until 9 to 16 weeks p.i. It is also possible that T cells are important for suppressing replication of persistent MAV-1. These two roles for T cells are not mutually exclusive. T cells have been shown to be important for protection against persistent viral infections (35, 54). For example, humans with specific T-cell deficiencies (e.g., DiGeorge syndrome and X-linked lymphoproliferative syndrome) are susceptible to productive infections of viruses that are normally persistent (4, 15, 16, 22). MAV-1 establishes persistent infections in outbred mice (reviewed in reference 64). In B6 mice, persistent MAV-1

DNA and mRNA were detected at 12 weeks p.i. (Fig. 5). It is not known whether the E3 mRNA detected in B6 spleens and brains at this time represents low-level chronic replication or whether MAV-1 can establish a latent phase in which E3 is transcribed. Sublethal irradiation of outbred mice persistently infected with MAV-1 results in increased levels of MAV-1 DNA (63). This suggests that replication of persistent MAV-1 is controlled by an immune mechanism.

Different T-cell subsets and effector functions can mediate immunopathology and viral clearance in various virus-host systems (19). However, the signals and events leading to differential T-cell responses to viruses remain poorly understood. Since the immune system evolved to counter a variety of pathogens, comparative viral pathogenesis aids our understanding of innate and adaptive immunity. Both $CD4^+$ and $CD8^+$ T cells have been shown to contribute to pathology in Sindbis virus (58), lymphocytic choriomeningitis virus (77), Borna disease virus (57), and mouse hepatitis virus (74) infections in mice, although the relative contributions of $CD4^+$ and $CD8^+$ T cells to pathology vary among these systems. Perforin-deficient mice have been shown to be resistant to acute disease induced by lymphocytic choriomeningitis virus (37), Murray Valley encephalitis virus (47), coxsackievirus B (21), cowpox virus (53), and MAV-1 (this report), but they are susceptible to acute ectromelia virus infection (53). It is likely that factors such as the cell type(s) infected and mode of virus replication determine T-cell responses to viruses (76). Like MAV-1, Hantaan virus targets macrophage/monocyte cells and endothelial cells (78), and its pathogenesis bears similarity to that of MAV-1. Both viruses establish persistent infections in mice, their natural host (18, 64), and both viruses cause acute encephalitis in adult B6 mice that is characterized by perivascular edema (compare Fig. 2 in this report to reference 71). Infection of athymic nude mice with Hantaan virus resulted in prolonged virus replication, compared to rapid clearance in BALB/c controls (3). These observations parallel results reported here. Macrophages and endothelial cells are both APCs that are known to express MHC class I and MHC class II molecules (1). Many viruses infect APCs; this strategy enables modulation of the host immune response, systemic dissemination, and viral persistence (19). Adenoviruses infect endothelial cells of many animal species, including cattle, moose, dog, cat, deer, chicken, pig, and 12 species of reptiles (41, 42, 55, 61, 65, 67, 69, 73). Our understanding of host immune responses will benefit from comparison of pathogenesis phenotypes induced by different viruses with similar target cell types.

We are pursuing identification of T-cell-dependent functions required for clearance of replicating MAV-1 and for survival of MAV-1 infection, such as the role of Fas ligand in T-cell-dependent clearance of MAV-1. Preliminary evidence indicates that the cytokine interferon gamma contributes to early protection but is dispensable for MAV-1 clearance and long-term host survival (Moore and Spindler, unpublished data).

T cells are known to be involved in immune responses to natural and experimental hAd infections (reviewed in reference 30). In acute pediatric upper respiratory disease caused by hAds, a significant increase in T cells and NK cells was observed, leading Matsubara et al. (49) to suggest that increased T-cell activation may be a useful parameter for determining the severity of adenovirus infection. It is likely that T cells contribute to disease severity in acute hAd infections. CMI causes disease in the context of many acute viral infections in animal models (13, 46, 47, 58), and T cells are implicated in acute immunopathology in human viral disease (17). Also, in murine and primate models of hAd-mediated gene therapy, T cells are a primary cause of inflammation and cellular damage (75, 80). These observations suggest that T-cell immunopathology may be a general component of both human and mouse adenovirus-induced disease.

ACKNOWLEDGMENTS

We thank Gwen Hirsch, Adriana Kajon, Carla Pretto, James Stanton, Brian Waters, and Amanda Welton for technical assistance. We thank Keith Bishop, Lei Fang, Gary Huffnagle, Michael Imperiale, Steve Kunkel, and Rick Tarleton for critical reviews of the manuscript.

This work was supported by NIH grant R01 AI023762 to K.R.S. and by an NIH predoctoral traineeship (GM 07103) and an ARCS Foundation Scholarship to M.L.M.

REFERENCES

1. **Abbas, A. K., A. H. Lichtman, and J. S. Pober.** 2000. Cellular and molecular immunology, 4th ed. W. B. Saunders Co., Philadelphia, Pa.
2. **Appay, V., J. J. Zaunders, L. Papagno, J. Sutton, A. Jaramillo, A. Waters, P. Easterbrook, P. Grey, D. Smith, A. J. McMichael, D. A. Cooper, S. L. Rowland-Jones, and A. D. Kelleher.** 2002. Characterization of CD4(+) CTLs ex vivo. J. Immunol. **168:**5954–5958.
3. **Asada, H., M. Tamura, K. Kondo, Y. Okuno, Y. Takahashi, Y. Dohi, T. Nagai, T. Kurata, and K. Yamanishi.** 1987. Role of T lymphocyte subsets in protection and recovery from Hantaan virus infection in mice. J. Gen. Virol. **68:**1961–1969.
4. **Asamoto, H., and M. Furuta.** 1977. Di George syndrome associated with glioma and two kinds of viral infection. N. Engl. J. Med. **296:**1235.
5. **Ball, A. O., C. W. Beard, P. Villegas, and K. R. Spindler.** 1991. Early region 4 sequence and biological comparison of two isolates of mouse adenovirus type 1. Virology **180:**257–265.
6. **Beard, C. W., and K. R. Spindler.** 1996. Analysis of early region 3 mutants of mouse adenovirus type 1. J. Virol. **70:**5867–5874.
7. **Bendelac, A., D. Killeen, D. R. Littman, and R. H. Schwartz.** 1994. A subset of CD4+ thymocytes selected by MHC class I molecules. Science **263:**1774–1778.
8. **Berk, A. J., F. Lee, T. Harrison, J. Williams, and P. A. Sharp.** 1979. Pre-early adenovirus 5 gene product regulates synthesis of early viral messenger RNAs. Cell **17:**935–944.
9. **Cauthen, A. N., and K. R. Spindler.** 1999. Construction of mouse adenovirus type 1 mutants, p. 85–103. *In* W. S. M. Wold (ed.), Adenovirus methods and protocols. Humana Press, Totowa, N.J.
10. **Charles, P. C., X. Chen, M. S. Horwitz, and C. F. Brosnan.** 1999. Differential chemokine induction by the mouse adenovirus type-1 in the central nervous system of susceptible and resistant strains of mice. J. Neurovirol. **5:**55–64.
11. **Charles, P. C., J. D. Guida, C. F. Brosnan, and M. S. Horwitz.** 1998. Mouse adenovirus type-1 replication is restricted to vascular endothelium in the CNS of susceptible strains of mice. Virology **245:**216–228.
12. **Chen, Y. H., N. M. Chiu, M. Mandal, N. Wang, and C. R. Wang.** 1997. Impaired NK1+ T cell development and early IL-4 production in CD1-deficient mice. Immunity **6:**459–467.
13. **Cole, G. A., N. Nathanson, and R. A. Prendergast.** 1972. Requirement for theta-bearing cells in lymphocytic choriomeningitis virus-induced central nervous system disease. Nature **238:**335–337.
14. **Coutelier, J.-P., P. G. Coulie, P. Wauters, H. Heremans, and J. T. M. van der Logt.** 1990. In vivo polyclonal B-lymphocyte activation elicited by murine viruses. J. Virol. **64:**5383–8388.
15. **Deerojanawong, J., A. B. Chang, P. A. Eng, C. F. Robertson, and A. S. Kemp.** 1997. Pulmonary diseases in children with severe combined immune deficiency and DiGeorge syndrome. Pediatr. Pulmonol. **24:**324–330.
16. **Dutz, J. P., L. Benoit, X. Wang, D. J. Demetrick, A. Junker, D. de Sa, and R. Tan.** 2001. Lymphocytic vasculitis in X-linked lymphoproliferative disease. Blood **97:**95–100.
17. **Ennis, F. A., J. Cruz, C. F. Spiropoulou, D. Waite, C. J. Peters, S. T. Nichol, H. Kariwa, and F. T. Koster.** 1997. Hantavirus pulmonary syndrome: CD8+ and CD4+ cytotoxic T lymphocytes to epitopes on Sin Nombre virus nucleocapsid protein isolated during acute illness. Virology **238:**380–390.
18. **Feuer, R., J. D. Boone, D. Netski, S. P. Morzunov, and S. C. St. Jeor.** 1999. Temporal and spatial analysis of Sin Nombre virus quasispecies in naturally infected rodents. J. Virol. **73:**9544–9554.
19. **Flint, S. J., L. W. Enquist, R. M. Krug, V. R. Racaniello, and A. M. Skalka.**

2000. Principles of virology: molecular biology, pathogenesis, and control. American Society for Microbiology, Washington, D.C.
20. **Garcia-Sanz, J. A., G. Plaetinck, F. Velotti, D. Masson, J. Tschopp, H. R. MacDonald, and M. Nabholz.** 1987. Perforin is present only in normal activated Lyt2+ T lymphocytes and not in L3T4+ cells, but the serine protease granzyme A is made by both subsets. EMBO J. **6:**933–938.
21. **Gebhard, J. R., C. M. Perry, S. Harkins, T. Lane, I. Mena, V. C. Asensio, I. L. Campbell, and J. L. Whitton.** 1998. Coxsackievirus B3-induced myocarditis: perforin exacerbates disease, but plays no detectable role in virus clearance. Am. J. Pathol. **153:**417–428.
22. **Gilger, M. A., D. O. Matson, M. E. Conner, H. M. Rosenblatt, M. J. Finegold, and M. K. Estes.** 1992. Extraintestinal rotavirus infections in children with immunodeficiency. J. Pediatr. **120:**912–917.
23. **Grusby, M. J., R. S. Johnson, V. E. Papaioannou, and L. H. Glimcher.** 1991. Depletion of $CD4^+$ T cells in major histocompatibility complex class II-deficient mice. Science **253:**1417–1420.
24. **Guida, J. D., G. Fejer, L.-A. Pirofski, C. F. Brosnan, and M. S. Horwitz.** 1995. Mouse adenovirus type 1 causes a fatal hemorrhagic encephalomyelitis in adult C57BL/6 but not BALB/c mice. J. Virol. **69:**7674–7681.
25. **Guidotti, L. G., and F. V. Chisari.** 2000. Cytokine-mediated control of viral infections. Virology **273:**221–227.
26. **Guidotti, L. G., R. Rochford, J. Chung, M. Shapiro, R. Purcell, and F. V. Chisari.** 1999. Viral clearance without destruction of infected cells during acute HBV infection. Science **284:**825–829.
27. **Hartley, J. W., and W. P. Rowe.** 1960. A new mouse virus apparently related to the adenovirus group. Virology **11:**645–647.
28. **Hausmann, J., W. Hallensleben, J. C. De La Torre, A. Pagenstechier, C. Zimmermann, H. Pircher, and P. Staeheli.** 1999. T cell ignorance in mice to Borna disease virus can be overcome by peripheral expression of the viral nucleoprotein. Proc. Natl. Acad. Sci. USA **96:**9769–9774.
29. **Hayday, A. C.** 2000. γ/δ cells: a right time and a right place for a conserved third way of protection. Annu. Rev. Immunol. **18:**975–1026.
30. **Horwitz, M. S.** 2001. Adenoviruses, p. 2301–2326. *In* D. M. Knipe and P. M. Howley (ed.), Fields virology, 4th ed., vol. 2. Lippincott Williams & Wilkins, Philadelphia, Pa.
31. **Inada, T., and H. Uetake.** 1978. Nature and specificity of effector cells in cell-mediated cytolysis of mouse adenovirus-infected cells. Infect. Immun. **22:**119–124.
32. **Inada, T., and H. Uetake.** 1978. Cell-mediated immunity assayed by ^{51}Cr release test in mice infected with mouse adenovirus. Infect. Immun. **20:**1–5.
33. **Inada, T., and H. Uetake.** 1978. Cell-mediated immunity to mouse adenovirus infection: macrophage migration inhibition test. Microbiol. Immunol. **22:**391–401.
34. **Inada, T., and H. Uetake.** 1980. Cell-mediated immunity to mouse adenovirus infection: blocking of macrophage migration inhibition and T cell-mediated cytolysis of infected cells by anti-S antigen or anti-alloantigen serum. Microbiol. Immunol. **24:**525–535.
35. **Iwashiro, M., K. Peterson, R. J. Messer, I. M. Stromnes, and K. J. Hasenkrug.** 2001. $CD4^+$ T cells and gamma interferon in the long-term control of persistent Friend retrovirus infection. J. Virol. **75:**52–60.
36. **Kaech, S. M., E. J. Wherry, and R. Ahmed.** 2002. Effector and memory T-cell differentiation: implications for vaccine development. Nat. Rev. Immunol. **2:**251–262.
37. **Kagi, D., B. Ledermann, K. Burki, P. Seiler, B. Odermatt, K. J. Olsen, E. R. Podack, R. M. Zinkernagel, and H. Hengartner.** 1994. Cytotoxicity mediated by T cells and natural killer cells is greatly impaired in perforin-deficient mice. Nature **369:**31–37.
38. **Kagi, D., B. Ledermann, K. Burki, R. M. Zinkernagel, and H. Hengartner.** 1996. Molecular mechanisms of lymphocyte-mediated cytotoxicity and their role in immunological protection and pathogenesis in vivo. Annu. Rev. Immunol. **14:**207–232.
39. **Kajon, A. E., C. C. Brown, and K. R. Spindler.** 1998. Distribution of mouse adenovirus type 1 in intraperitoneally and intranasally infected adult outbred mice. J. Virol. **72:**1219–1223.
40. **Kaplan, M. M., T. J. Wiktor, and H. Koprowski.** 1975. Pathogenesis of rabies in immunodeficient mice. J. Immunol. **114:**1761–1765.
41. **Kelly, W. R.** 1993. The liver and biliary system, p. 239–312. *In* K. V. F. Jubb, P. C. Kennedy, and N. Palmer (ed.), Pathology of domestic animals, 4th ed. Academic Press, San Diego, Calif.
42. **Kennedy, F. A., and T. P. Mullaney.** 1993. Disseminated adenovirus infection in a cat. J. Vet. Diagn. Investig. **5:**273–276.
43. **Kimura, T., and D. E. Griffin.** 2000. The role of $CD8^+$ T cells and major histocompatibility complex class I expression in the central nervous system of mice infected with neuroadapted Sindbis virus. J. Virol. **74:**6117–6125.
44. **Koller, B. H., P. Marrack, J. W. Kappler, and O. Smithies.** 1990. Normal development of mice deficient in β2M, MHC class I proteins, and $CD8^+$ T cells. Science **248:**1227–1230.
45. **Kring, S. C., C. S. King, and K. R. Spindler.** 1995. Susceptibility and signs associated with mouse adenovirus type 1 infection of adult outbred Swiss mice. J. Virol. **69:**8084–8088.
46. **Lane, T. E., M. T. Liu, B. P. Chen, V. C. Asensio, R. M. Samawi, A. D. Paoleti, I. L. Campbell, S. L. Kunkell, H. S. Fox, and M. J. Buchmeier.** 2000. A central role for $CD4^+$ T cells and RANTES in virus-induced central nervous system inflammation and demyelination. J. Virol. **74:**1415–1424.
47. **Licon Luna, R. M., E. Lee, A. Mullbacher, R. V. Blanden, R. Langman, and M. Lobigs.** 2002. Lack of both Fas ligand and perforin protects from flavivirus-mediated encephalitis in mice. J. Virol. **76:**3202–3211.
48. **Makino, Y., D. N. Cook, O. Smithies, O. Y. Hwang, E. G. Neilson, L. A. Turka, H. Sato, A. D. Wells, and T. M. Danoff.** 2002. Impaired T cell function in RANTES-deficient mice. Clin. Immunol. **102:**302–309.
49. **Matsubara, T., T. Inoue, N. Tashiro, K. Katayama, T. Matsuoka, and S. Furukawa.** 2000. Activation of peripheral blood CD8+ T cells in adenovirus infection. Pediatr. Infect. Dis. **19:**166–768.
50. **Meissner, J. D., G. N. Hirsch, E. A. LaRue, R. A. Fulcher, and K. R. Spindler.** 1997. Completion of the DNA sequence of mouse adenovirus type 1: Sequence of E2B, L1, and L2 (18–51 map units). Virus Res. **51:**53–64.
51. **Miller, G., S. Lahrs, V. G. Pillarisetty, A. B. Shah, and R. P. DeMatteo.** 2002. Adenovirus infection enhances dendritic cell immunostimulatory properties and induces natural killer and T-cell-mediated tumor protection. Cancer Res. **62:**5260–5266.
52. **Mombaerts, P., A. R. Clarke, M. A. Rudnicki, J. Iacomini, S. Itohara, J. J. Lafaille, L. Wang, Y. Ichikawa, R. Jaenisch, M. L. Hooper, and S. Tonegawa.** 1992. Mutations in T-cell antigen receptor genes α and β block thymocyte development at different stages. Nature **360:**225–231.
53. **Mullbacher, A., R. T. Hla, C. Museteanu, and M. Simon.** 1999. Perforin is essential for control of ectromelia virus but not related poxviruses in mice. J. Virol. **73:**1665–1667.
54. **Murray, P. D., K. D. Pavelko, J. Leibowitz, X. Lin, and M. Rodriguez.** 1998. $CD4^+$ and $CD8^+$ T cells make discrete contributions to demyelination and neurologic disease in a viral model of multiple sclerosis. J. Virol. **72:**7320–7329.
55. **Perkins, L. E., R. P. Campagnoli, B. G. Harmon, C. R. Gregory, W. L. Steffens, K. Latimer, S. Clubb, and M. Crane.** 2001. Detection and confirmation of reptilian adenovirus infection by in situ hybridization. J. Vet. Diagn. Investig. **13:**365–368.
56. **Pirofski, L., M. S. Horwitz, M. D. Scharff, and S. M. Factor.** 1991. Murine adenovirus infection of SCID mice induces hepatic lesions that resemble human Reye syndrome. Proc. Natl. Acad. Sci. USA **88:**4358–4362.
57. **Planz, O., T. Bilzer, and L. Stitz.** 1995. Immunopathogenic role of T-cell subsets in Borna disease virus-induced progressive encephalitis. J. Virol. **69:**896–903.
58. **Rowell, J. F., and D. E. Griffin.** 2002. Contribution of T cells to mortality in neurovirulent Sindbis virus encephalomyelitis. J. Neuroimmmunol. **127:**106–114.
59. **Scott, B., H. Bluthmann, H. S. Teh, and H. von Boehmer.** 1989. The generation of mature T cells requires interaction of the alpha beta T-cell receptor with major histocompatibility antigens. Nature **338:**591–593.
60. **Sha, Z., and R. W. Compans.** 2000. Induction of $CD4^+$ T-cell-independent immunoglobulin responses by inactivated influenza virus. J. Virol. **74:**4999–5005.
61. **Shilton, C. M., D. A. Smith, L. W. Woods, G. J. Crawshaw, and H. D. Lehmkuhl.** 2002. Adenoviral infection in captive moose (*Alces alces*) in Canada. J. Zool. Wildl. Med. **33:**73–79.
62. **Shinkai, Y., K. Takio, and K. Okumura.** 1988. Homology of perforin to the ninth component of complement (C9). Nature **334:**525–527.
63. **Smith, K., C. C. Brown, and K. R. Spindler.** 1998. The role of mouse adenovirus type 1 early region 1A in acute and persistent infections in mice. J. Virol. **72:**5699–5706.
64. **Smith, K., and K. R. Spindler.** 1999. Murine adenovirus, p. 477–484. *In* R. Ahmed and I. Chen (ed.), Persistent viral infections. John Wiley & Sons, New York, N.Y.
65. **Smyth, J. A., D. A. Moffett, E. van Garderen, and J. P. Orr.** 1999. Examination of adenovirus-types in intestinal vascular endothelial inclusions in fatal cases of enteric disease in cattle, by in situ hybridisation. Vet. Microbiol. **70:**1–6.
66. **Spindler, K. R., L. Fang, M. L. Moore, C. C. Brown, G. N. Hirsch, and A. K. Kajon.** 2001. SJL/J mice are highly susceptible to infection by mouse adenovirus type 1. J. Virol. **75:**12039–12046.
67. **Tang, K. N., C. A. Baldwin, J. L. Mansell, and E. L. Styer.** 1995. Disseminated adenovirus infection associated with cutaneous and visceral hemorrhages in a nursing piglet. Vet. Pathol. **32:**433–437.
68. **van der Veen, J., and A. Mes.** 1973. Experimental infection with mouse adenovirus in adult mice. Arch. Gesamte Virusforsch. **42:**235–241.
69. **Veit, H. P., C. H. Domermuth, and W. B. Gross.** 1981. Histopathology of avian adenovirus group II splenomegaly of chickens. Avian Dis. **25:**866–873.
70. **Wang, B., C. C. Norbury, R. Greenwood, J. R. Bennink, J. W. Yewdell, and J. A. Frelinger.** 2001. Multiple paths for activation of naive CD8+ T cells: CD4-independent help. J. Immunol. **167:**1283–1289.
71. **Wichmann, D., H.-J. Grone, M. Frese, J. Pavlovic, B. Anheier, O. Haller, H.-D. Klenk, and H. Feldman.** 2002. Hantaan virus infection causes acute neurological disease that is fatal in adult laboratory mice. J. Virol. **76:**8890–8899.

72. **Williams, N. S., and V. H. Engelhard.** 1996. Identification of a population of CD4+ CTL that utilizes a perforin- rather than a Fas ligand-dependent cytotoxic mechanism. J. Immunol. **156:**153–159.
73. **Woods, L. W., R. S. Hanley, P. H. Chiu, M. Burd, R. W. Nordhausen, M. H. Stillian, and P. K. Swift.** 1997. Experimental adenovirus hemorrhagic disease in yearling black-tailed deer. J. Wildl. Dis. **33:**801–811.
74. **Wu, G. F., A. A. Dandekar, L. Pewe, and S. Perlman.** 2000. CD4 and CD8 T cells have redundant but not identical roles in virus-induced demyelination. J. Immunol. **165:**2278–2286.
75. **Yang, Y., Q. Li, H. C. J. Ertl, and J. M. Wilson.** 1995. Cellular and humoral immune responses to viral antigens create barriers to lung-directed gene therapy with recombinant adenoviruses. J. Virol. **69:**2004–2015.
76. **Zajac, A. J., J. M. Dye, and D. G. Quinn.** 2003. Control of lymphocytic choriomeningitis virus infection in granzyme B deficient mice. J. Virol. **305:** 1–9.
77. **Zajac, A. J., D. G. Quinn, P. L. Cohen, and J. A. Frelinger.** 1996. Fas-dependent CD4+ cytotoxic T-cell-mediated pathogenesis during virus infection. Proc. Natl. Acad. Sci. USA **93:**14730–14735.
78. **Zaki, S. R., P. W. Greer, L. M. Coffield, C. S. Goldsmith, K. B. Nolte, K. Foucar, R. M. Feddersen, R. E. Zumwalt, G. L. Miller, and A. S. Khan.** 1995. Hantavirus pulmonary syndrome. Pathogenesis of an emerging infectious disease. Am. J. Pathol. **146:**552–579.
79. **Zinkernagel, R. M., and H. Hengartner.** 2001. Regulation of the immune response by antigen. Science **293:**251–253.
80. **Zotlick, P. W., N. Chirmule, M. A. Schnell, G.-P. Gao, J. V. Hughes, and J. M. Wilson.** 2001. Biology of E1-deleted adenovirus vectors in nonhuman primate muscle. J. Virol. **75:**5222–5229.